8508 *Inorg. Chem.* **2009**, *48*, 8508–8514
DOI: 10.1021/ic901293h

Inorganic Chemistry
Article

The Unique Palladium-Centered Pentagonal Antiprismatic Cationic Bismuth Cluster: A Comparison of Related Metal-Centered 10-Vertex Pnictogen Cluster Structures by Density Functional Theory

R. B. King,*,† I. Silaghi-Dumitrescu,‡ and M. M. Uţă‡

†*Department of Chemistry, University of Georgia, Athens, Georgia 30602, and* ‡*Faculty of Chemistry and Chemical Engineering, Babeş-Bolyai University, Cluj-Napoca, Roumania*

Received July 5, 2009

Structures for the metal-centered 10-vertex pnictogen clusters $M@Pn_{10}^{4+}$ (M = Ni, Pd, Pt; Pn = As, Sb, Bi) based on polyhedra with 3-fold, 4-fold, and 5-fold symmetry have been studied by density functional theory. Among these nine M/Pn combinations, only $Pd@Bi_{10}^{4+}$ and $Pt@Bi_{10}^{4+}$ are predicted to have the D_{5d} pentagonal antiprism as the lowest energy structure in accord with experimental observation of this cluster in the ternary halide $Bi_{14}PdBr_{10}$ as well as the prediction of the Wade−Mingos rules for these *arachno* systems. The lowest energy structures for the arsenic and antimony clusters $M@Pn_{10}^{4+}$ (Pn = As, Sb) and $Ni@Bi_{10}^{4+}$ are predicted to have structures derived from a tetracapped trigonal prism that has been severely distorted for $M@As_{10}^{4+}$ (M = Pd, Pt). The volumes of the As_{10} polyhedra other than the pentagonal prism are too small to contain interstitial palladium or platinum atoms so that major distortions are predicted for such clusters leading to partial opening of the polyhedron.

1. Introduction

Studies by Zintl and co-workers in the 1930s[1−4] on the potentiometric titrations of post-transition elements with alkali metals in liquid ammonia led to the discovery of a series of bare anionic clusters of the post-transition elements, including particularly group 14 and group 15 elements. The structures of many of these anionic clusters were determined by Corbett and co-workers in the 1960s after they found suitable counterions to isolate crystalline derivatives amenable to structure determination by X-ray diffraction.[5] Corbett and co-workers also characterized structurally a number of bare post-transition element cluster cations obtained in strongly Lewis acidic media.[6]

The original post-transition element clusters were empty clusters, that is, they contained no interstitial atoms in the center of the cluster polyhedron. However, subsequent synthetic studies led to the discovery of clusters containing interstitial transition metals. The synthetic studies of Ruck[7] are of particular interest since they led to the discovery of extensive series of bismuth clusters containing interstitial transition metal atoms. Among the clusters discovered by Ruck, a particularly interesting metal-centered bismuth cluster is the pentagonal antiprismatic $Pd@Bi_{10}^{4+}$ cation[8] found in the ternary halide $Bi_{14}PdBr_{10}$.

The initial bonding models for the post-transition element clusters were based on the isoelectronic and apparently isolobal nature of bare group 14 element vertices and BH vertices, as well as that of bare group 15 element vertices and CH vertices. Thus the Ge_n^{2-} clusters were regarded as analogues of the deltahedral boranes $B_nH_n^{2-}$ and thus were expected to have similar deltahedral structures according to the Wade−Mingos rules.[9−12] Using this approach the $Pd@Bi_{10}^{4+}$ cation is seen to be a 10-vertex *arachno* system with (2)(1) + 6 = 26 skeletal electrons in which the bare bismuth vertices each contribute 3 skeletal electrons but the interstitial palladium atom contributes zero skeletal electrons because of the stability of its filled d^{10} shell.[13] Such an *arachno* system with n vertices is expected to have two non-triangular faces or one large open face with a shape derived from a deltahedron with $n + 2$ vertices by removing two of the vertices and all of the edges associated with them. The pentagonal antiprism is obviously derived in this way from

*To whom correspondence should be addressed. E-mail: rbking@chem.uga.edu.

(1) Zintl, E.; Goubeau, J.; Dullenkopf, W. *Z. Phys. Chem., Abt. A* **1931**, *154*, 1.
(2) Zintl, E.; Harder, A. *Z. Phys. Chem., Abt. A* **1931**, *154*, 47.
(3) Zintl, E.; Dullenkopf, W. *Z. Phys. Chem., Abt. B* **1932**, *16*, 183.
(4) Zintl, E.; Kaiser, H. *Z. Anorg. Allgem. Chem.* **1933**, *211*, 113.
(5) Corbett, J. D. *Chem. Rev.* **1985**, *85*, 383.
(6) Corbett, J. D. *Prog. Inorg. Chem.* **1976**, *21*, 129.
(7) Ruck, M. *Angew. Chem., Int. Ed.* **2001**, *40*, 1182.
(8) Ruck, M.; Dubenskyy, V.; Söhnel, T. *Angew. Chem., Int. Ed.* **2003**, *42*, 2978.
(9) Wade, K. *Chem. Commun.* **1971**, 792.
(10) Wade, K. *Adv. Inorg. Chem. Radiochem.* **1976**, *18*, 1.
(11) Mingos, D. M. P. *Acc. Chem. Res.* **1984**, *17*, 311.
(12) Mingos, D. M. P.; Johnston, R. L. *Struct. Bonding (Berlin)* **1987**, *68*, 29.
(13) King, R. B. *Dalton Trans.* **2004**, 3420.

 Published on Web 08/07/2009

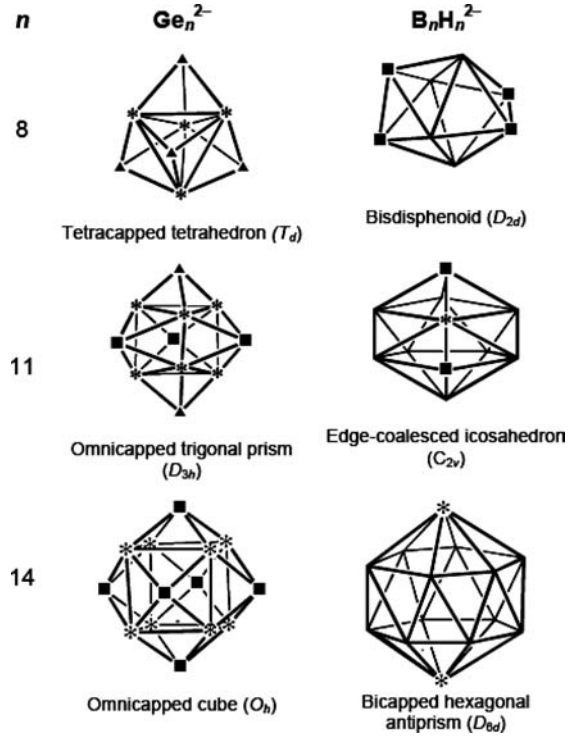

Figure 1. Examples of different lowest energy structures for isoelectronic Ge_n^{2-} and $B_nH_n^{2-}$ derivatives (n = 8, 11, 14). Degree 6, 4, and 3 vertices are indicated by *, ■, and ▲, respectively, and degree 5 vertices are unmarked.

an icosahedron by removing an antipodal pair of vertices leading to two pentagonal faces and D_{5d} point group symmetry.

For this reason the pentagonal antiprismatic structure of $Pd@Bi_{10}^{4+}$ originally did not appear to be particularly unusual. However, density functional theory (DFT) studies on bare germanium clusters in our group[14−19] indicated that in some cases the favored deltahedra for the bare Ge_n^{2-} clusters are completely different from those of the corresponding deltahedral boranes (Figure 1). This suggested that the Wade−Mingos rules[9−12] are not necessarily applicable in bare post-transition element clusters as had been previously believed. Alternatively stated, the "external" lone pairs in the bare post-transition element clusters are not truly external lone pairs but participate in the skeletal bonding. Our subsequent work[20] showed that the jellium model of physicists[21,22] can be applied to bare post-transition element clusters and, in particular, indicated that a total of 40 valence electrons is a "magic number" for special cluster stability. This accounted for the prevalence of 40 total valence electron

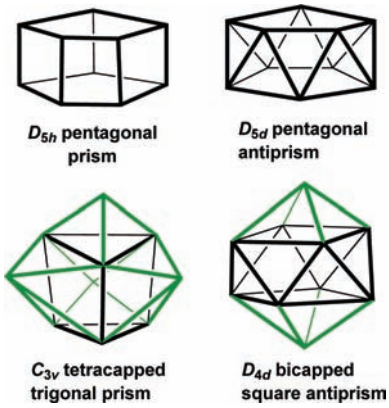

Figure 2. 10-Vertex polyhedra with three-, four-, and five-fold symmetry used as starting structures in these theoretical studies.

clusters such as In_{11}^{7-}, $Ni@In_{10}^{10-}$, and Ge_9^{4-} as products from the synthesis of bare post-transition element clusters under forcing conditions, such as high temperature reactions.

The 10-vertex post-transition element cluster systems also attracted our attention for another reason, namely, the experimental realization of stable structures based on different 10-vertex polyhedra representing examples of 3-fold, 4-fold, and 5-fold symmetry (Figure 2). In this connection the isoelectronic systems $Ni@In_{10}^{10-}$ and $Zn@In_{10}^{8-}$ were found experimentally to exhibit structures having different 10-vertex deltahedra, namely the D_{4d} bicapped square antiprism for $Zn@In_{10}^{8-}$ (ref 23) but a C_{3v} polyhedron for $Ni@In_{10}^{10-}$ (ref 24). These experimental results were consistent with our theoretical results,[25] which, however, used the isoelectronic germanium clusters $Ni@Ge_{10}$ and $Zn@Ge_{10}^{2+}$ to model the indium clusters to avoid the computational and other problems associated with the high negative charges on the indium clusters. Furthermore, for none of the related 26-skeletal electron 10-vertex germanium clusters in this study, namely, $Ni@Ge_{10}^{6-}$, $Cu@Ge_{10}^{5-}$, and $Zn@Ge_{10}^{4-}$, was the pentagonal antiprism predicted to be the preferred structure. In addition, experimental work reported within the past year has led to the discovery of the Zintl ion cages $M@Ge_{10}^{3-}$ (M = Fe,[26] Co[27]) containing the transition metal in the center of a pentagonal prismatic Ge_{10} cluster without any triangular faces at all. Such pentagonal prismatic clusters are not predicted by any plausible application of the Wade−Mingos rules.[9−12] These observations all suggest that the experimentally known[8] $Pd@Bi_{10}^{4+}$ cation is a more special system than had been previously realized since its pentagonal antiprismatic structure is unusual among bare post transition element clusters, whether or not they contain interstitial atoms.

To investigate further the relative stabilities of different 10-vertex polyhedra as cages for interstitial atoms, we have now extended our theoretical studies to include the following nine systems $M@Pn_{10}^{4+}$ (M = Ni, Pd, Pt; Pn = As, Sb, Bi). A striking observation from this work, reported in detail in this paper, is that the $Pd@Bi_{10}^{4+}$ and $Pt@Bi_{10}^{4+}$ systems

(14) King, R. B.; Silaghi-Dumitrescu, I.; Kun, A. *Dalton Trans.* **2002**, 3999.
(15) King, R. B.; Silaghi-Dumitrescu, I. *Inorg. Chem.* **2003**, *42*, 6701.
(16) King, R. B.; Silaghi-Dumitrescu, I.; Lupan, A. *Inorg. Chem.* **2005**, *44*, 3579.
(17) King, R. B.; Silaghi-Dumitrescu, I.; Lupan, A. *Dalton Trans.* **2005**, 1858.
(18) King, R. B.; Silaghi-Dumitrescu, I.; Uţă, M. M. *Inorg. Chem.* **2006**, *45*, 4974.
(19) King, R. B.; Silaghi-Dumitrescu, I.; Uţă, M. M. *Dalton Trans.* **2007**, 364.
(20) King, R. B.; Silaghi-Dumitrescu, I. *Dalton Trans.* **2008**, 6083.
(21) De Heer, W. A. *Rev. Mod. Phys.* **1993**, *65*, 611.
(22) Janssens, E.; Neukermans, S.; Lievens, P. *Curr. Opin. Solid State Mater. Sci.* **2004**, *8*, 185.
(23) Sevov, S. C.; Corbett, J. C. *Inorg. Chem.* **1993**, *32*, 1059.
(24) Henning, R. W.; Corbett, J. D. *Inorg. Chem.* **1999**, *38*, 3883.
(25) King, R. B.; Silaghi-Dumitrescu, I.; Uţă, M. M. *Chem. Eur. J.* **2008**, *14*, 4542.
(26) Zhou, B.; Denning, M. S.; Kays, D. L.; Goicoechea, J. M. *J. Am. Chem. Soc.* **2009**, *132*, 2802.
(27) Wang, J.-Q.; Stegmaier, S.; Fässler, T. F. *Angew Chem., Int. Ed.* **2009**, *48*, 1998.

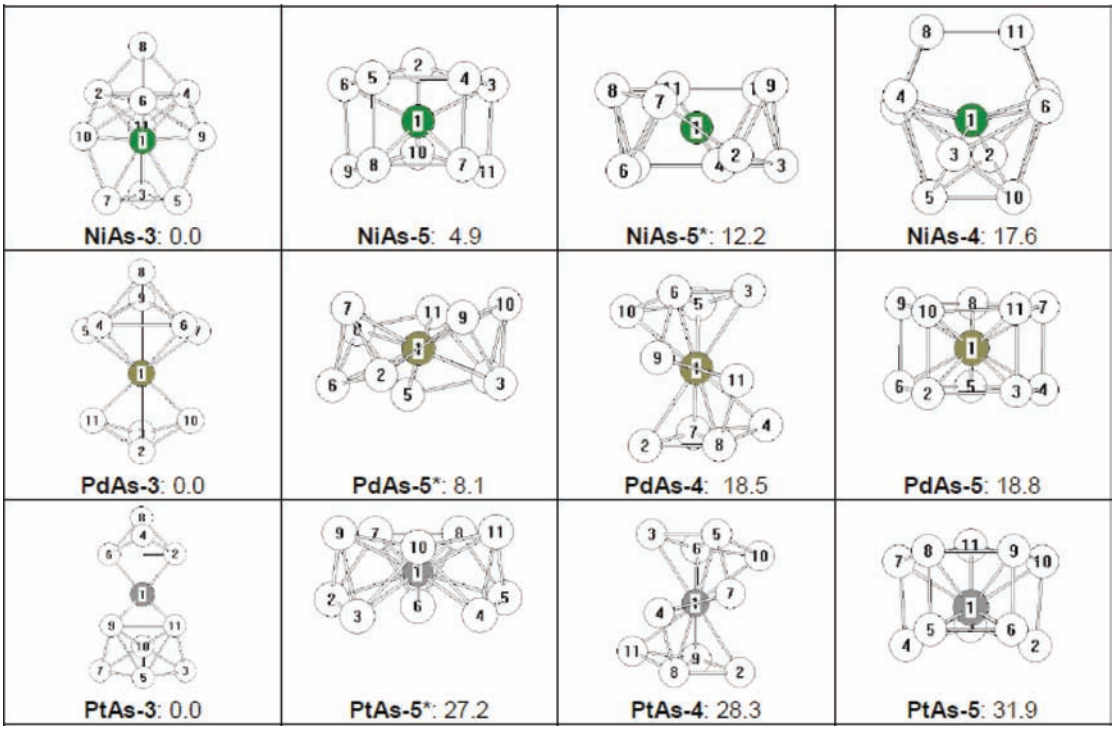

Figure 3. Structures of the $M@As_{10}^{4+}$ clusters (M = Ni, Pd, Pt) with relative energies in kcal/mol.

are the only ones of these nine systems for which the pentagonal antiprismatic structure is predicted to be the lowest energy structure. Furthermore, structures based on a pentagonal prism with no triangular faces, similar to those recently found experimentally for $M@Ge_{10}^{3-}$ (M = Fe,[26] Co[27]), are found to be low-energy structures for a number of these systems.

2. Computational Methods

Geometry optimizations were carried out at the hybrid DFT B3LYP level[28−31] using ECP LANL2DZ basis sets with one additional f type polarization function (LANL08) for the interstitial atoms (Ni, Pd, Pt).[32] The ECP LANL2DZd basis sets[33] with one additional d polarization function were used for the pnictogen cluster atoms (As, Sb, Bi). The Gaussian 03 package of programs[34] was used in which the fine grid (75,302) is the default for numerically evaluating the integrals and the tight (10^{-8}) hartree stands as default for the self-consistent field convergence. Computations were carried out using four initial geometries including 10-vertex polyhedra with 3-fold, 4-fold, and 5-fold symmetry (Figure 2). The symmetries were maintained during the initial geometry optimization processes. Symmetry breaking using modes defined by imaginary vibrational frequencies was then used to determine the minimum energy optimized structures. Vibrational analyses show that all of the final optimized structures discussed in this paper are genuine minima at the B3LYP/LANL2DZ level without any significant imaginary frequencies ($N_{imag} = 0$). In a few cases the calculations ended with acceptable small imaginary frequencies[35] and these values are indicated in the corresponding figures.

The optimized structures found for the $M@Pn_{10}^{4+}$ clusters (M = Ni, Pd, Pt; Pn = As, Sb, Bi) (Figures 3, 4, and 5) are labeled by the central metal atom (Ni, Pd, Pt) followed by the pnictogen cluster atom (As, Sb, Bi). Since in several instances the initial symmetry was changed by following normal modes corresponding to imaginary vibrational frequencies, we do not use the point group symbol but rather indicate the order of the principal rotation axis of the starting structure. Thus, **5** and **5*** differentiate between the D_{5h} pentagonal prism and the D_{5d} pentagonal antiprism, respectively. Triplet structures are indicated by **T**. Thus the pentagonal antiprismatic structure of singlet $Pd@Bi_{10}^{4+}$ is labeled **PdBi-5*** Additional details of all of the optimized structures, including all interatomic distances and the initial geometries leading to a given optimized structure, are provided in the Supporting Information.

3. Results and Discussion

Figures 3 to 5 show the optimized structures of the $M@Pn_{10}^{4+}$ derivatives (M = Ni, Pd, Pt; Pn = As, Sb, Bi) in order of relative energies, indicated in kcal/mol. The global minima for all of the $M@As_{10}^{4+}$ and $M@Sb_{10}^{4+}$ clusters (Figures 3 and 4: M = Ni, Pd, Pt) and $Ni@Bi_{10}^{4+}$ originate from the tetracapped trigonal prisms **MAs-3**, **MSb-3**, and **NiBi-3** with various degrees of distortion from the ideal C_{3v} structures. Since the volume of the As_{10} cluster is the smallest, the **AsPn-3** clusters undergo the most severe deformations from ideal C_{3v} symmetry. Thus, the C_{3v} symmetry $Ni@As_{10}^{4+}$ structure is a third order stationary point on the energy hypersurface. Following the corresponding normal

(28) Vosko, S. H.; Wilk, L.; Nusair, M. *Can. J. Phys.* **1980**, *58*, 1200.
(29) Lee, C.; Yang, W.; Parr, R. G. *Phys. Rev. B* **1988**, *37*, 785.
(30) Becke, A. D. *J. Chem. Phys.* **1993**, *98*, 5648.
(31) Stephens, P. J.; Devlin, F. J.; Chabalowski, C. F.; Frisch, M. J. *J. Phys. Chem.* **1994**, *98*, 11623.
(32) Roy, L. E.; Hay, P. J.; Martin, R. L. *J. Chem. Theory Comput.* **2008**, *4*, 1029.
(33) Check, C. E.; Faust, T. O.; Bailey, J. M.; Wright, B. J.; Gilbert, T. M.; Sunderlin, L. S. *J Phys. Chem. A* **2001**, *105*, 8111.
(34) Frisch, M. J. et al. *Gaussian 03*, Revision C 02; Gaussian, Inc.: Wallingford, CT, 2004 (see Supporting Information for details).
(35) Xie, Y.; Schaefer, H. F.; King, R. B. *J. Am. Chem. Soc.* **2000**, *122*, 8746.

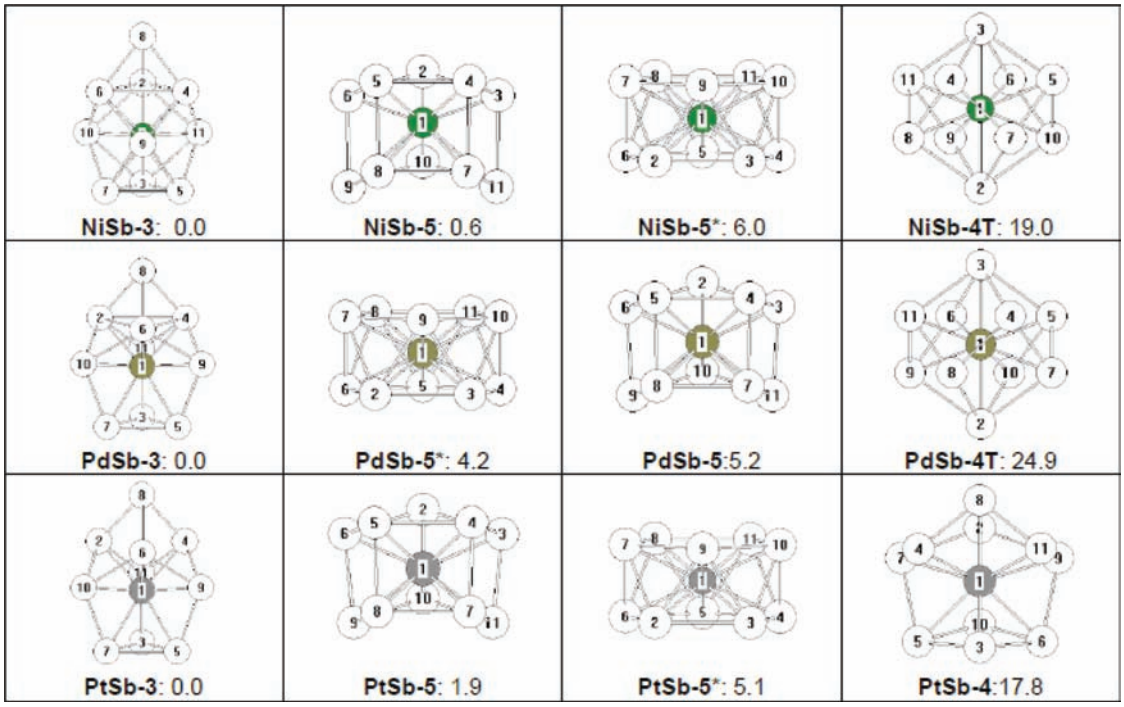

Figure 4. Structures of the $M@Sb_{10}^{4+}$ clusters (M = Ni, Pd, Pt) with relative energies in kcal/mol.

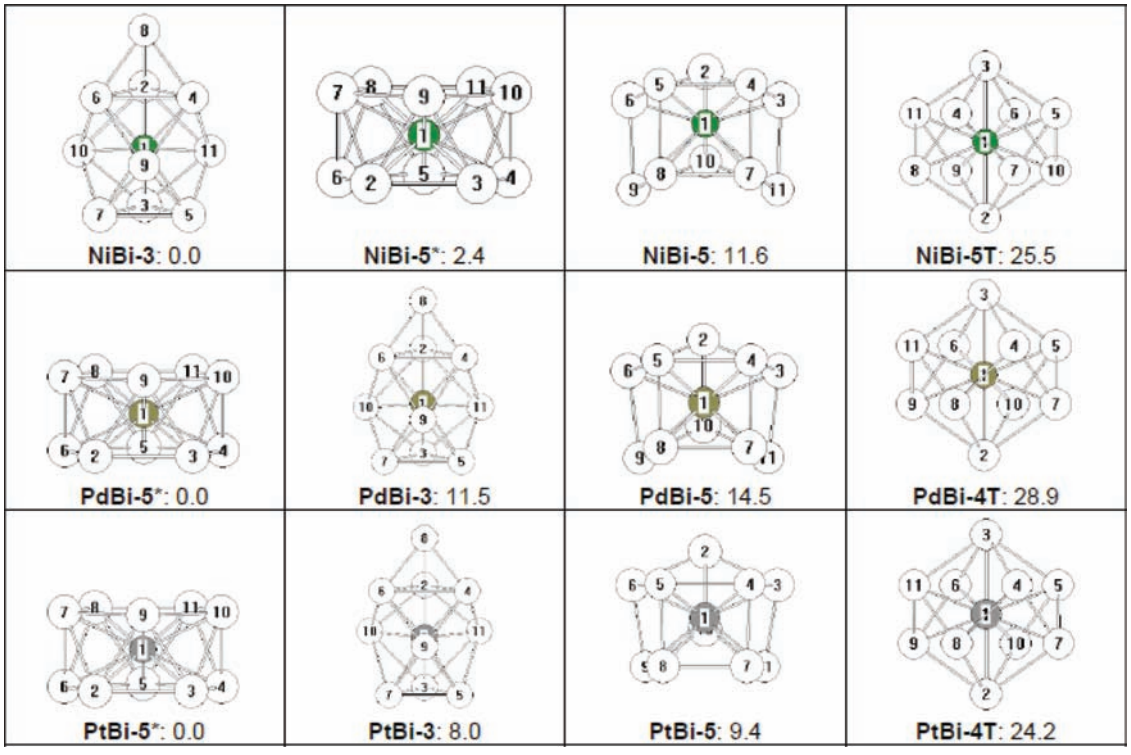

Figure 5. Structures of the $M@Bi_{10}^{4+}$ clusters (M = Ni, Pd, Pt) with relative energies in kcal/mol.

modes leads to a minimum with C_3 symmetry and to a C_s configuration 8.9 kcal/mol higher in energy (see the Supporting Information). The underlying polyhedron of the C_3 symmetry cluster is related to an octahedron, elongated along the C_3 axis. This octahedron is formed by rotation of one of the triangular faces of the original trigonal prism by 60°. One of the Ni−As distances in **NiAs-3** (3.46 Å) is much longer than the other nine (3 × 2.46 Å, 3 × 2.52 Å, 3 × 2.61 Å). This is consistent with the fact that the nine orbitals of the sp^3d^5 manifold of the group 10 atom are not sufficient to form two-electron two-center bonds with all 10 of the As atoms.

The global minima for the $M@As_{10}^{4+}$ clusters (M = Pd, Pt) are open C_s symmetry polyhedra derived from the C_{3v} structure (Figure 3), since an As_{10} tetracapped trigonal prism is too small to accommodate the Pd and Pt atoms. The effect

Table 1. Dimensions of Pentagonal Antiprismatic Metal Clusters[a]

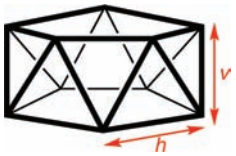

cluster	v	h	v/h[b]	M@Pn_{10} distance	APT charge
{Ni@As_{10}^{4+}}	2.60	2.80	0.93	2.61	−0.573
{Pd@As_{10}^{4+}}	2.60	2.94	0.88	2.71	−0.619
{Pt@As_{10}^{4+}}	2.58	2.95	0.87	2.72	−0.754
Ni@Sb_{10}^{4+}	3.01	3.09	0.97	2.92	−0.447
Pd@Sb_{10}^{4+}	3.00	3.18	0.94	2.98	−0.489
Pt@Sb_{10}^{4+}	2.99	3.18	0.94	2.98	−0.568
Ni@Bi_{10}^{4+}	3.11	3.18	0.98	3.00	−0.429
Pd@Bi_{10}^{4+}	3.11	3.25	0.96	3.05	−0.454
Pt@Bi_{10}^{4+}	3.11	3.25	0.96	3.05	−0.515
Pd@Bi_{10}^{4+} (expt)	3.15	3.16	1.00	3.00	

[a] Distances in Å. Structures in braces {} have small imaginary frequencies and collapse to the structures in the figures upon following the corresponding normal modes. [b] v/h = 0.97(As), 0.98(Sb), 1.02(Bi) for the empty Pn_{10}^{4+} clusters.

of size matching is observed for $NiSb_{10}^{4+}$ and $NiBi_{10}^{4+}$ where the lowest energy structures exhibit the full C_{3v} symmetry of the tetracapped trigonal prism. Thus, the global minimum for the nickel-centered bismuth cluster Ni@Bi_{10}^{4+}, namely, **NiBi-3** (Figure 5), is a C_{3v} polyhedron in which nine of the Ni−Bi distances are much shorter than the tenth Ni−Bi distance to the unique bismuth atom on the C_3 axis. The nickel atom in **NiBi-3** thus may be regarded as nine-coordinate with distorted tricapped trigonal prismatic geometry. This is consistent with sp^3d^5 hybridization of the central nickel atom in **NiBi-3**. For the (Pd or Pt)@Sb_{10}^{4+} global minima **PdSb-3** and **PtSb-3** the symmetry is again reduced to C_3 to allow more space for the central atom.

The situation is very different for the platinum and palladium-centered bismuth clusters (Pd or Pt)@Bi_{10}^{4+} (**PdBi-5*** and **PtBi-5*** in Figure 5) than for the other seven {Ni,Pd,Pt}/{As,Sb,Bi} combinations. Thus the global minimum structures for the two clusters M@Bi_{10}^{4+} (M = Pd, Pt) are not based on the C_{3v} tetracapped trigonal prism but instead are centered D_{5d} pentagonal antiprisms, consistent with the experimental data[8] on $Bi_{14}PdBr_{10}$. The C_{3v} structures for Pd@Bi_{10}^{4+} and Pt@Bi_{10}^{4+} lie 11.5 and 8.0 kcal/mol, respectively, above the corresponding D_{5h} pentagonal antiprismatic global minima (Figure 5).

The pentagonal antiprismatic M@Pn_{10}^{4+} clusters of ideal D_{5d} symmetry have two distinct Pn−Pn distances, namely, the "horizontal" distances h and the "vertical" distances v (Table 1). For the six pentagonal antiprismatic M@Pn_{10}^{4+} (Pn = Sb, Bi) that are genuine minima, the v/h ratios fall in the range 0.94 to 1.00 (compared with 0.97 to 1.02 calculated for the empty clusters optimized to D_{5d} geometry). The three pentagonal antiprismatic clusters M@As_{10}^{4+} (M = Ni, Pd, Pt) are not genuine minima but instead are higher order stationary points (HOS) with significant imaginary vibrational frequencies (see the Supporting Information). The configurations corresponding to the HOS have lower v/h ratios in the range 0.87 to 0.93 and are unstable toward lengthening some of the As−As edges of the pentagonal antiprism leading to a more open structure. Apparently the volume of an As_{10} pentagonal antiprism with "vertical" edges v of ∼2.60 Å and "horizontal" edges h of ∼2.80 to 2.90 Å (Table 1) is not large enough to accommodate an interstitial platinum or palladium atom of radius 1.39 Å or 1.36 Å, or even the smaller nickel atom (of radius 1.24 Å), without significant distortion of the original polyhedron.

The atomic polar tensor (APT) charges[36] on M (M = Ni, Pd, Pt) listed in the last column of Table 1 show an increase from Ni to Pt for all the pnictogen cages and decrease for the same interstitial metal by going from As_{10} to Bi_{10}. If M is considered to be a d^{10} electron metal, then higher charge transfer from the Pn_{10} cage leads to greater destabilization of the electron configuration of the central atom. Therefore, the highest charges are encountered for the As_{10} cages, where, owing to the spatial congestion, the largest amount of charge on the transition metals is encountered. This leads to increased distortion as indicated by the lowest v/h ratio for {Pt@As_{10}^{4+}}.

Relevant geometrical parameters for the C_{3v} tetracapped trigonal prism are given in Table 2. The v/h ratio (h is the mean value of the horizontal edge of the underlying trigonal prism and v is the length of the vertical edge) is taken as a measure of the distortion of the polyhedron from the ideal shape given by the geometry of the empty Pn_{10}^{4+} optimized to C_{3v} symmetry. An initial observation is that the edges of the capped triangular faces of the underlying tricapped trigonal prism (h_c in Table 2) are lengthened from 3.2 Å to 3.8 Å so that they no longer correspond to significant Pn−Pn interactions. Thus, the resulting polyhedron can be considered to have 3 quadrilateral and 10 triangular faces rather than the original 16 triangular faces of a 10-vertex deltahedron such as a tetracapped trigonal prism.

All six of the M@Pn_{10}^{4+} C_{3v} symmetry based structures (M = Ni, Pd, Pt; Pn = Sb, Bi) have nine of the Pn atoms within bonding distance of the central metal atom at 2.6 to 3.0 Å (Table 2). However, the remaining M−Pn distance to the Pn vertex on the C_3 axis is significantly longer at 4.16 ± 0.04 Å, which clearly corresponds to a non-bonding distance. The nine M−Pn bonds at the vertices of a distorted tricapped trigonal prism correspond to sp^3d^5 hybrids formed by the valence orbitals of the interstitial metal atom M.

Optimization of the C_{3v} M@As_{10}^{4+} clusters (M = Ni, Pd, Pt) suggests that a C_{3v} As_{10} tetracapped trigonal prism does not have a large enough cavity to hold the central interstitial metal atom M. Moreover the APT charges (Table 2) are higher than for those found for the pentagonal antiprismatic structures (Table 1), suggesting a greater destabilization of the d^{10} configuration. Thus all three of the initially optimized C_{3v} M@As_{10}^{4+} clusters (M = Ni, Pd, Pt) maintaining the original C_{3v} symmetry have imaginary vibrational frequencies. Following the corresponding normal modes destroys the C_{3v} symmetry in all three cases. For Ni@As_{10}^{4+} (**NiAs-3**) this distortion is relatively high since it reduces the energy of the structure by 17.7 kcal/mol making it the global minimum for this system. For the corresponding palladium- and platinum-centered As_{10} clusters the corresponding distortion reduces the energy by a much larger amount, namely, 89.3 kcal/mol for Pd@As_{10}^{4+} and 22.6 kcal/mol for Pt@As_{10}^{4+}.

(36) Cioslowski, J. *J. Am. Chem. Soc.* **1989**, *111*, 8333.

Table 2. Dimensions of Tetracapped Trigonal Prismatic Metal Clusters[a]

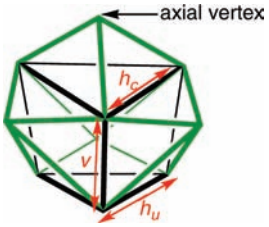

cluster	v	h_c	h_u	Δh	$\bar{h}$	$v/\bar{h}$[b]	M@Pn_{10} distances[c]	APT charge
{Ni@As_{10}^{4+}}	3.81	3.42	2.66	0.76	3.04	1.25	2.43(3), 2.64(3), 2.66(3), 3.64(1)	−0.735
{Pd@As_{10}^{4+}}	4.37	3.50	2.62	0.88	3.06	1.42	2.53(3), 2.79(3), 2.84(3), 3.81(1)	−0.727
{Pt@As_{10}^{4+}}	4.40	3.52	2.62	0.90	3.07	1.43	2.54(3), 2.81(3), 2.86(3), 3.80(1)	−0.819
Ni@Sb_{10}^{4+}	4.22	3.71	3.05	0.66	3.38	1.25	2.67(3), 2.87(3), 2.89(3), 4.12(1)	−0.536
{Pd@Sb_{10}^{4+}}	4.44	3.85	3.02	0.83	3.43	1.29	2.75(3), 2.97(3), 3.00(3), 4.12(1)	−0.538
{Pt@Sb_{10}^{4+}}	4.44	3.85	3.02	0.83	3.43	1.29	2.75(3), 2.97(3), 3.00(3), 4.12(1)	−0.630
Ni@Bi_{10}^{4+}	4.26	3.71	3.18	0.53	3.44	1.24	2.73(3), 2.90(3), 2.94(3), 4.20(1)	−0.359
Pd@Bi_{10}^{4+}	4.33	3.86	3.20	0.66	3.53	1.23	2.83(3), 2.96(3), 3.00(3), 4.12(1)	−0.336
Pt@Bi_{10}^{4+}	4.43	3.91	3.15	0.76	3.53	1.25	2.81(3), 3.00(3), 3.03(3), 4.18(1)	−0.474

[a] Distances in Å. Structures in braces {} have small imaginary frequencies and collapse to the structures in the figures upon following the corresponding normal modes. [b] v/h = 1.36(As), 1.32(Sb), 1.32(Bi) for the empty Pn_{10}^{4+} clusters. [c] The figures in parentheses indicate the numbers of equivalent M−Pn distances.

Furthermore, the original topology of the C_{3v} tetracapped trigonal prism is not recognizable in the final structure.

The other polyhedron found consistently for the M@Pn_{10}^{4+} systems (M = Ni, Pd, Pt; Pn = As, Sb, Bi) is based on the pentagonal prism of D_{5h} symmetry. The significance of such structures has increased since the synthesis and characterization of the endohedral pentagonal prismatic M@Ge_{10}^{3-} (M = Fe,[26] Co[27]) clusters during the past year. The pentagonal prismatic structure is energetically available, lying less than 5.2 kcal/mol higher than the global minima for M@Sb_{10}^{4+} and less than 15 kcal/mol for M@Bi_{10}^{4+}. While for M@As_{10}^{4+} (M=Ni, Pd, Pt) the vertical/horizontal distance ratios (v/h) are 0.95, 0.93, and 0.92, respectively, for the other six pentagonal prisms M@Sb_{10}^{4+} and M@Bi_{10}^{4+} this ratio is 0.96 to 0.97. This is very close to the experimental value of 0.97 for the M@Ge_{10}^{3-} (M = Fe,[26] Co[27]) clusters. This suggests that the higher compressions of the Pd@As_{10}^{4+} and Pt@As_{10}^{4+} clusters lead to their higher relative energies. For the antimony and bismuth clusters, the compression of the pentagonal prism cluster leads to lower relative energies, as noted above.

A fourth structure type found for the M@Pn_{10}^{4+} derivatives (M = Ni, Pd, Pt; Pn = As, Sb, Bi) is the bicapped square antiprism. These structures have triplet spin multiplicity. The six structures M@Sb_{10}^{4+} and M@Bi_{10}^{4+} with full D_{4d} symmetry (M = Ni, Pd, Pt; Figures 4 and 5) have no imaginary vibrational frequencies and are thus genuine minima. However, these structures lie 18 to 30 kcal/mol above the corresponding global minima and are thus the highest energy optimized structures found in this work.

The arsenic systems obtained by optimization of the M@As_{10}^{4+} D_{4d} bicapped square antiprism starting structures, although still triplets, are again anomalous because of the smaller internal volume of the As_{10} bicapped square antiprism relative to the corresponding Sb_{10} and Bi_{10} polyhedra. The bicapped square antiprismatic cluster As_{10} containing the smaller interstitial nickel atom is not a minimum on the potential surface. Following the normal modes of the imaginary vibrational frequencies gives **NiAs-4** (Figure 3) as the lowest energy cluster originating from the D_{4d} symmetry structure. The corresponding D_{4d} Pd@As_{10}^{4+} and Pt@As_{10}^{4+} structures also exhibit three to five imaginary vibrational frequencies, respectively. Following the corresponding normal modes lengthens some of the As−As distances and lowers the energy leading to the relatively opened structures **PdAs-4** and **PtAs-4** (Figure 3). These results indicate that an As_{10} bicapped square antiprism, like some of the other As_{10} polyhedra studied in this work, is not large enough to accommodate a palladium or platinum atom without some distortion.

4. Summary

Since the interstitial group 10 metals Ni, Pd, Pt can be regarded as donors of zero skeletal electrons because of their filled d^{10} shells,[13] the 10-vertex systems M@Pn_{10}^{4+} (M = Ni, Pd, Pt; Pn = As, Sb, Bi) correspond to 26 skeletal electron systems with each pnictogen vertex donating three skeletal electrons leaving an external lone pair on each vertex. The Wade−Mingos rules[9−12] predict *arachno* structures for these clusters. The most obvious *arachno* structure is the D_{5d} pentagonal antiprism (Figure 2 and Table 1), derived from an icosahedron by removal of an antipodal pair of vertices. Such a pentagonal antiprismatic *arachno* structure is found as the lowest energy structure only for Pd@Bi_{10}^{4+} and Pt@Bi_{10}^{4+} (**PdBi-5*** and **PtBi-5*** in Figure 5). Interestingly enough, Pd@Bi_{10}^{4+} is the only M@Pn_{10}^{4+} (M = Ni, Pd, Pt; Pn = As, Sb, Bi) derivative known experimentally.[8] Furthermore, the experimental Pd@Bi_{10}^{4+} structure is indeed the pentagonal antiprism predicted by our theoretical work to be our lowest energy structure. The corresponding D_{5d} pentagonal antiprismatic structure for Ni@Bi_{10}^{4+} (**NiBi-5***), although not the global minimum, is still a relatively low energy structure, lying only 6.4 kcal/mol above the corresponding global minimum **NiBi-3**.

The predicted lowest energy structures for the arsenic and antimony clusters $M@Pn_{10}^{4+}$ (Pn = As, Sb) and $Pt@Bi_{10}^{4+}$ are derived from a tetracapped trigonal prism that has been severely distorted for $M@As_{10}^{4+}$ (M = Pd, Pt). In this connection, the As_{10} polyhedra have significantly smaller volumes than the corresponding Sb_{10} and Bi_{10} polyhedra since the arsenic covalent radius is only 1.19 Å as compared with covalent radii of 1.39 Å and 1.48 Å for antimony and bismuth, respectively. For this reason interstitial palladium atoms (radius 1.39 Å) or platinum atoms (radius 1.36 Å) in the As_{10} polyhedra, other than the maximum volume pentagonal prism, lead to severe distortions that make the original polyhedron essentially unrecognizable (Figure 3).

Acknowledgment. We are indebted to the National Science Foundation for support of this work under Grant CHE-0716718. Part of this work was undertaken with financial support from the CMMCCC 130/2007 program, Romania.

Supporting Information Available: Table S1: $Ni@As_{10}^{4+}$ optimized structures; Table S2, $Pd@As_{10}^{4+}$ optimized structures; Table S3, $Pt@As_{10}^{4+}$ optimized structures; Table S4, $Ni@Sb_{10}^{4+}$ optimized structures; Table S5, $Pd@Sb_{10}^{4+}$ optimized structures; Table S6, $Pt@Sb_{10}^{4+}$ optimized structures; Table S7, $Ni@Bi_{10}^{4+}$ optimized structures; Table S8, $Pd@Bi_{10}^{4+}$ optimized structures; Table S9, $Pt@Bi_{10}^{4+}$ optimized structures; Complete Gaussian03 reference (reference 34). This material is available free of charge via the Internet at http://pubs.acs.org.